AIAA JOURNAL
Vol. 48, No. 9, September 2010

Technical Notes

Impact of Harmonic Perturbations on a Turbulent Mixing Layer

Yuli Lifshitz* and David Degani†
Technion–Israel Institute of Technology, Haifa 32000, Israel

DOI: 10.2514/1.J050470

Nomenclature

A	=	flap amplitude
i	=	$\sqrt{-1}$
f	=	frequency, Hz
S_{kj}	=	strain-rate tensor of time-averaged motion
$\tilde{s}_{kj}$	=	strain-rate tensor of harmonic motion
U, $\bar{u}$	=	time-averaged value
$\langle u \rangle$	=	phase-averaged value
$\tilde{u}$	=	coherent part of the phase-averaged value
u_k	=	x_k component of instantaneous velocity
u'_k	=	x_k velocity component of random motion
x_k	=	Cartesian coordinates
α	=	complex wave number
θ	=	momentum thickness
ν_T	=	eddy viscosity
τ_{kj}	=	part of Reynolds stress tensor caused by random pulsations
$\tilde{\tau}_{kj}$	=	part of Reynolds stress tensor caused by harmonic motion
ω	=	circular frequency

Subscripts

k, j, n	=	vector and tensor components, Fourier mode number

Superscript

$*$	=	complex-conjugate value

Introduction

THIS Note presents a theory explaining a puzzling phenomenon revealed in experimental studies of Oster and Wygnanski [1] and Weisbrot and Wygnanski [2] regarding a turbulent mixing layer with imposed harmonic perturbations. In the experiments, the mixing layer between parallel streams of different velocities past a splitter plate was excited by an oscillating flap located at the end of the splitter plate. Three distinct regions were distinguished in the streamwise development of the mixing layer. In region I, the growth rate of the forced mixing layer exceeded its unforced linear growth. In region II, the growth rate slowed down or stopped. Finally, in region III, the mixing layer resumed its downstream growth at about the unforced rate. The shear component of Reynolds stresses was also calculated using measured instantaneous velocity fields. In region II this stress becomes manyfold smaller than in the undisturbed mixing layer. The Reynolds stress consists of two parts: coherent Reynolds stress (CRS) caused by harmonic motion and turbulent Reynolds stress (TRS) caused by random pulsations. Because the CRS may be negative, Reau and Tumin [3] attributed the diminishing of the Reynolds stress in region II to the negative values of CRS. However their estimation was not accurate enough and the more accurate theory of Lifshitz et al. [4] showed that the TRS in region II must be manyfold smaller than in the unforced mixing layer as well. This brings up a question: What is the mechanism of coherent–random interaction that results in such a drastic diminishing of the TRS? In the present Note we answer this question using our calculations of [4] and the results of Wygnanski and Weisbrot [5], who showed that the Kelvin–Helmholtz waves are likely to generate the TRS.

Governing Equations

Any turbulent flow can be decomposed into a mean and fluctuating component by introducing an average used for deriving the Reynolds-averaged Navier–Stokes (RANS) equations. The idea of the triple decomposition is to further divide the fluctuating component into a coherent and a random part. In the case of artificial harmonic perturbation with a given frequency f, it is possible to introduce a phase average, taking the period of the perturbation as the characteristic timescale. The phase-averaged parameters are further divided into the time-averaged and the coherent parts, where the latter is represented as a sum of Fourier modes of the forcing frequency. For example, the velocity component u_k ($k = 1, 2, 3$) is recast as

$$u_k = \langle u_k \rangle + u'_k, \qquad \langle u_k \rangle = U_k + \tilde{u}_k,$$
$$\tilde{u}_k = \frac{1}{2}\sum_n (\tilde{u}_{k,n} e^{-2i\pi nft} + \tilde{u}^*_{k,n} e^{2i\pi nft}) \tag{1}$$

Substituting the velocity components and the pressure in the form of Eq. (1) into the Navier–Stokes equations and time-averaging leads to the RANS-type equations of the time-averaged flow in tensor notation (the index summation rule is imposed):

$$\frac{\partial U_k}{\partial x_k} = 0, \qquad \frac{\partial U_k U_j}{\partial x_j} + \frac{\partial P}{\partial x_k} = \frac{\partial \tau_{kj}}{\partial x_j} + \frac{\partial \tilde{\tau}_{kj}}{\partial x_j} \tag{2}$$

Here, the laminar viscosity is neglected, $\tau_{kj} = -\overline{u'_k u'_j}$ represents a time-averaged part of the TRS tensor (in the presence of the coherent perturbation), and $\tilde{\tau}_{kj}$ is the CRS arising from the coherent part of Eq. (1):

$$\tilde{\tau}_{kj} = -\frac{1}{4}\sum_n (\tilde{u}_{k,n}\tilde{u}^*_{j,n} + \tilde{u}_{j,n}\tilde{u}^*_{k,n}) \tag{3}$$

Substituting the velocity and the pressure in the form of Eq. (1) into the Navier–Stokes equations, phase-averaging and subtraction of Eq. (2) results in RANS-type equations for the amplitude of the nth mode:

$$\frac{\partial \tilde{u}_{k,n}}{\partial x_k} = 0,$$
$$-2i\pi nf\tilde{u}_{k,n} + U_j\frac{\partial \tilde{u}_{k,n}}{\partial x_j} + \tilde{u}_{j,n}\frac{\partial U_k}{\partial x_j} + \frac{\partial \tilde{p}_n}{\partial x_k} = \frac{\partial r_{kj,n}}{\partial x_j} + \frac{\partial \tilde{\tau}_{kj,n}}{\partial x_j} \tag{4}$$

Here, $r_{kj,n}$ stands for the nth mode of the term $r_{kj} = \overline{u'_k u'_j} - \langle u'_k u'_j \rangle$, which is responsible for the dissipation of a coherent signal by the

Received 17 February 2010; revision received 29 June 2010; accepted for publication 2 July 2010.

*Research Associate, Department of Mechanical Engineering.
†Professor, Department of Mechanical Engineering, Associate Fellow AIAA.

random field, the bar denotes a time-averaging, and $\tilde{\tau}_{kj,n}$ arises from the nonlinear interaction of the modes.

Now one has to adopt a closure approximation for τ_{kj} and the harmonics of r_{kj} in Eqs. (2) and (4), respectively. According to their definitions, both tensors can be calculated if the approximation of Reynolds stresses, $\tau_{kj} + r_{kj} = -\langle u'_k u'_j \rangle$, is known. Various closure schemes were considered by Reynolds and Hussain [6]. The simplest is the quasi-laminar model, $r_{kj} = 0$, which means that $\langle u'_k u'_j \rangle = \overline{u'_k u'_j}$ and any interaction between the coherent and the random parts of flow is neglected. Reau and Tumin [3] showed that this model is very coarse; it overestimates the overall growth of coherent disturbances in a turbulent mixing layer by two- and threefold in comparison with experimental data of Gaster et al. [7]. To allow for the coherent–random interaction, Reynolds and Hussain [6] proposed the Newtonian model, $r_{kj} = 2\tilde{\nu}_T \tilde{s}_{kj}$, which relates the Reynolds stress oscillations to $\tilde{s}_{kj}$ through a scalar eddy viscosity. The same form of closure is taken for the time-averaged Reynolds stresses. This means that

$$\tau_{kj} = 2\nu_T S_{kj}, \qquad r_{kj,n} = 2\tilde{\nu}_T \tilde{s}_{kj,n} \tag{5}$$

Only shear stress component τ_{12} is considered as important for a two-dimensional mean field of turbulent thin shear layer, and the simplest hypothesis, $\tilde{\nu}_T = \nu_T$, is used for calculations of the coherent part of flow. Lifshitz et al. [4] provided comparison with experimental data that indicated a good potential of Eq. (5) for weak harmonic waves in several types of shear layers and in the mixing layer in particular. In the case of a turbulent mixing layer between streams with velocities V_1 and $V_2 (V_1 > V_2)$ along the x_1 axis, the eddy viscosity is modeled by a Prandtl-type algebraic formula:

$$\nu_T(x_1) = \chi\theta(x_1)(V_1 - V_2) \tag{6}$$

where χ is an experimentally defined constant and

$$\theta = \int_{-\infty}^{+\infty} \frac{U_1 - V_2}{V_1 - V_2}\left(1 - \frac{U_1 - V_2}{V_1 - V_2}\right) \mathrm{d}x_2 \tag{7}$$

Although the eddy viscosity is a constant in x_2 direction, Eq. (6) gives good self-similar results, better in comparison with the conventional k-ε turbulence model [8], and therefore Eq. (6) is usually used for such problems.

Discussion

The mathematical problem as a whole is solved by iterating the mean-flow solution of Eq. (2) for a given CRS and the coherent-flow solution of Eq. (4) for a given mean-velocity field U_k and ν_T. Thin-layer approximation is used for the mean flow, whereas the coherent-flow problem is transformed to full equations for stream function and vorticity to be solved by a finite difference scheme. Several results are presented in [4] for the mixing layer, the far wake, and a boundary layer subjected to a highly adverse pressure gradient together with additional details of the numerical methods and their validation. Here, we concentrate on the mixing layer between parallel streams with velocities V_1 and V_2 past a splitter plate excited by an oscillating flap at its end. This flow was studied experimentally [1,2] for a wide range of frequencies and amplitudes of the oscillated flap and for several values of $r = V_2/V_1$. Calculations in [4] demonstrate two key features of the flow. The first one is the interaction between the mean part of flow and the coherent wave generated by the flap. The CRS caused by the wave distorts the mean-velocity field, which in turn impacts the wave development. As a result, a finite amplitude wave begins to attenuate much upstream than infinitesimal one. This is shown in Fig. 1 by calculations of forced turbulent mixing layer, carried out for conditions $V_1 = 13.5$ m/s, $V_2 = 0.6V_1$, $f = 40$ Hz, and flap amplitude $A = 1.5$ mm used in the experiment of [1]. This set of parameters is referred in the caption of Fig. 1 and below as the Oster–Wygnanski (OW) conditions.

Taking into account the bell shape of $\tilde{\tau}_{12}(x_1, x_2)$ in cross sections of the mixing layer with a maximum near the centerline, the variation of $\tilde{\tau}_{12}(x_1, 0)$ is presented. A large difference between calculations

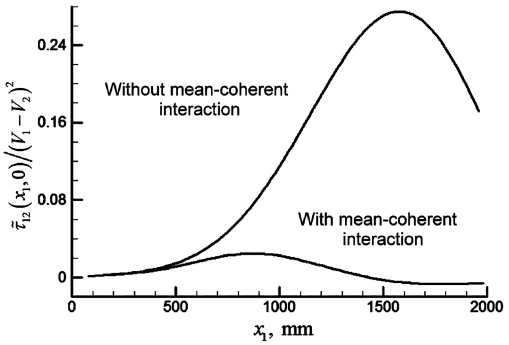

Fig. 1 Variation of the shear CRS component along the centerline of mixing layer between streams at the OW conditions.

with and without mean-coherent interaction is clearly seen, although the mean-velocity distortion is relatively small. This meets the well-known hypersensitivity of Eq. (4) to variation of U_k. Propagating downstream in the mixing layer, a coherent wave grows upstream of the neutral stability curve and dies out downstream, so that a maximum of the wave amplitude is reached at the neutral stability point. Figure 1 shows that the mean-coherent interaction distorts the mean velocity in such a way that the wave becomes more stable: it shifts the neutral stability curve upstream and decreases the rate of growth.

The second feature is the essential decrease of the shear Reynolds stress in region II. Lifshitz et al. [4] associated this behavior with the coherent–random interaction and approximated it by using the following equation for the eddy viscosity:

$$\frac{\nu_{T0}}{\nu_T} = \frac{\theta_0}{\theta(x_1)} + C_T \frac{\nu_T}{\nu_{T0}} \frac{f x_1^2}{U_m^3} \int_{-\infty}^{\infty} \left|\frac{\partial \tilde{u}_1}{\partial x_2}\right|^2 \mathrm{d}x_2, \qquad U_m = \frac{V_1 + V_2}{2} \tag{8}$$

where subscript 0 relates to unforced flow, and $C_T > 0$ is a constant obtained from experiments. The first term on the right-hand side of Eq. (8) is the Prandtl algebraic eddy viscosity, and the second term allows the decrease of the eddy viscosity due to the coherent wave influence. This term includes the effect of frequency and wave amplitude combined according to the qualitative behavior of the experimental data [1] and the dimensional analysis. Figure 2 compares the calculated displacement thickness of Eq. (7) (solid lines) with experimental data of [1] (symbols) for the OW conditions. Only this quantity was chosen for comparison because it was presented in [1] for the whole range of studied flows. In region I ($x_1 < 900$), the high growth rate is mostly caused by the high CRS; thus, the results of the calculation with $C_T = 0$ and 0.36 are close to one another and conform to the experiment. Downstream in region II, the CRS is small and the impact of the coherent–random interaction becomes major. Neglecting the interaction ($C_T = 0$) leads to noticeable difference between the experimental and the computed data. The diminishing eddy viscosity at $C_T = 0.36$ brings them

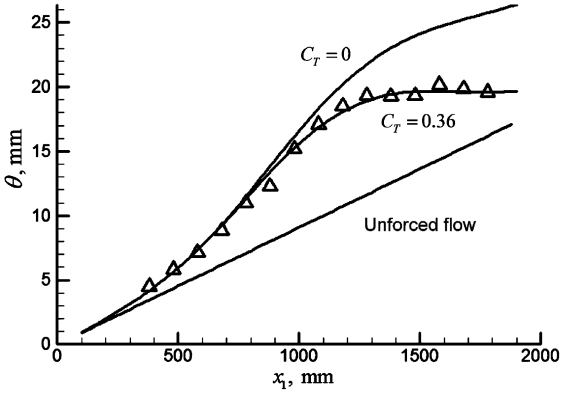

Fig. 2 Variation of momentum thickness at the OW conditions.

together. The use of Eq. (8) results in a satisfactory agreement with the experimental data of [1] not only for the OW conditions, but for the whole range of flows tested there. However, Eq. (8) does not explain the physics of the coherent–random interaction. Here, we present such an explanation.

The main part of the TRS is generated by large coherent structures, which are an intrinsic feature of a turbulent mixing layer. They were discovered using different techniques of flow visualization by Brown and Roshko [9] and Winant and Browand [10]. Flow visualization is very important for forming the notion of turbulent shear flows, but it seldom provides the quantitative data needed for understanding the processes involved. In the case of the mixing layer, the visualization formed a concept that the interface of mixing components rolls up into discrete vortices, which merge further into larger vortical structures supporting the divergence of the layer. Recently, Rikanati et al. [11] used this idea to estimate the visual growth of a turbulent mixing layer. They represented the interface as a set of discrete vortices and considered their merging caused by three-neighboring–vortex interactions in the initial flowfield. Studies of Wygnanski and Weisbrot [5] were based mostly on the measurements of the instantaneous flowfield, with further analysis of phase-locked and time-averaged characteristics. They investigated a plane turbulent mixing layer past a splitter plate disturbed by a small flap oscillating at a single frequency and at two frequencies: a fundamental and a subharmonic. The results are in rather poor agreement with the above concept, but they elucidate the key dynamical processes in the mixing layer.

We concentrate on the first part of this investigation relating to the phase-locked streakline pattern and to the phase-locked spanwise vorticity component. These results were obtained in [5] using two distinct methods: direct calculation based on the phase-locked velocity components and computation of the Kelvin–Helmholtz waves developing in a time-averaged divergent velocity field of the mixing layer. In quasi-parallel approximation the disturbances of pressure and velocity components of these waves in the form

$$\tilde{u}_k = e^{i(\alpha x_1 - \omega t)} \hat{u}_k(x_2/x_1), \qquad \alpha = \alpha_r + i\alpha_i \tag{9}$$

obey an eigenvalue problem. Its inviscid solution in the form of streakline patterns and vorticity contour maps in Figs. 1 and 2 of [5] showed good agreement with the phase-locked data. Wygnanski and Weisbrot [5] also claimed that their vorticity contours are very similar to those drawn by Browand and Weidman [12] based on conditionally sampled measurements in an unexcited mixing layer. One can conclude from these data that the large coherent structures of mixing layer are the Kelvin–Helmholtz waves, and eddies revealed by visualization are the vortex lumps emerging in the wave due to the roll-up of streaklines. The CRS of these waves produce the main part of the TRS.

A Kelvin–Helmholtz wave propagates downstream with phase velocity $(V_1 + V_2)/2$, and its growth or attenuation is completely determined by the time-averaged velocity and the eddy viscosity, which are coefficients of Eq. (4). The dynamics of the wave can be roughly estimated by the location of neutral stability curve. Figure 3 shows these curves and stable and unstable regions of undisturbed (self-similar) turbulent mixing layer with $V_1 = 13.5$ m/s and $V_2/V_1 = 0.6$ and of an identical mixing layer excited by flap oscillations with frequency $f = 40$ Hz and amplitude $A = 1.5$ mm. The calculations were carried out for the mean-velocity fields and ν_T of [4] using a quasi-parallel approximation and $\tilde{\nu}_T = \nu_T$. In coordinates $(x_1, 2\pi/\alpha_r)$ the neutral stability curve is a straight line for the case of undisturbed self-similar flow, but the curve has another form and is located farther upstream for the distorted velocity field of the excited mixing layer. This means that the wave amplitude begins to decrease father upstream in the excited flow than in the undisturbed one.

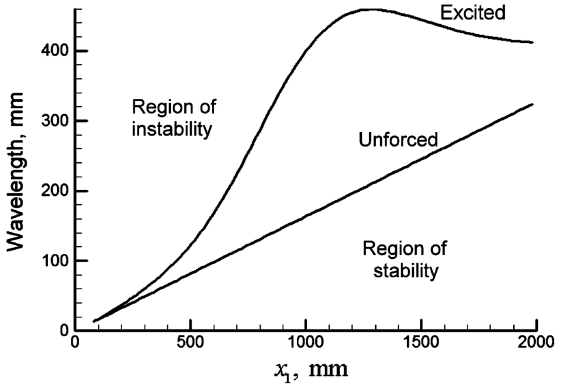

Fig. 3 Neutral stability curves for unforced and excited turbulent mixing layer at the OW conditions.

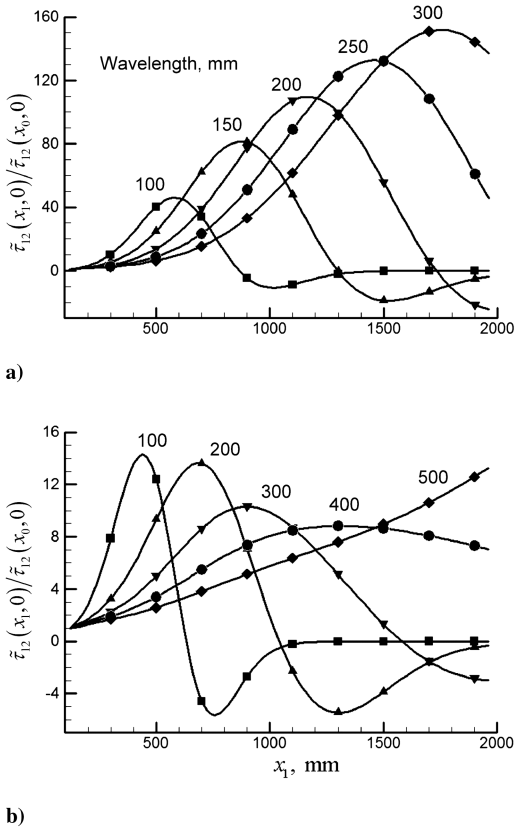

Fig. 4 Variation of the shear component of CRS generated by infinitesimal harmonic disturbances of different wavelengths: a) unforced flow and b) forced flow.

The CRS of the Kelvin–Helmholtz wave is defined by Eq. (3) with velocity components from a finite difference solution of Eq. (4) for a given mean-velocity field U_k and ν_T. Figure 4 shows variation of the shear stress component $\tilde{\tau}_{12}(x_1, x_2)$ generated by infinitesimal, noninteracting monochromatic perturbations of several wavelengths in the mixing layer at the OW conditions. The variation of the ratio $\tilde{\tau}_{12}(x_1, 0)/\tilde{\tau}_{12}(x_0, 0)$ well demonstrates the difference in the dynamics of coherent structures in the undisturbed and excited mixing layer (x_0 is the abscissa of the left boundary with given inflow conditions). One can conclude from the data presented in Fig. 4 that the distorted mean-velocity field of harmonically excited mixing layer suppresses the generation of the turbulent stress in comparison with the undisturbed flow. At the OW conditions, the computations show about a tenfold decrease of $\tilde{\tau}_{12}(x_1, x_2)$. This fact is reflected to some degree by Eq. (6), because the increase of $|\partial\tilde{u}_1/\partial x_2|$ in the second term of Eq. (6) decreases the eddy viscosity.

Conclusions

We have explained the mechanism of coherent–random interaction, provided that the large coherent structures are Kelvin–Helmholtz waves. This interaction is not a direct process; rather, it is a

two-stage one. In the first stage, a harmonic perturbation distorts the time-averaged streamwise velocity; in the second stage, the velocity distortion changes both the dynamics of the harmonic perturbation itself and of the large coherent structures. These structures are responsible for the Reynolds stress production. The distortion of the time-averaged velocity profile is usually small, but the crossflow derivative of the spanwise vorticity near the centerline may change significantly, causing noticeable variation of the stability features of the time-averaged flow and the behavior of large coherent structures, as shown in Figs. 3 and 4. We anticipate that the impact of harmonic perturbation on other types of shear layers is also determined by the distortion of the time-averaged velocity profile.

Acknowledgment

The authors would like to thank A. Tumin for useful discussions during the preparation of this work.

References

[1] Oster, D., and Wygnanski, I., "The Forced Mixing Layer Between Parallel Streams," *Journal of Fluid Mechanics*, Vol. 123, 1982, pp. 91–130.
doi:10.1017/S0022112082002973

[2] Weisbrot, I., and Wygnanski, I., "On Coherent Structures in a Highly Excited Mixing Layer," *Journal of Fluid Mechanics*, Vol. 195, 1988, pp. 137–159.
doi:10.1017/S0022112088002356

[3] Reau, N., and Tumin, A., "On Harmonic Perturbations in a Turbulent Mixing Layer," *European Journal of Mechanics, B/Fluids*, Vol. 21, 2002, pp. 143–155.
doi:10.1016/S0997-7546(01)01170-0

[4] Lifshitz, Y., Degani, D., and Tumin, A., "On the Interaction of Turbulent Shear Layers with Harmonic Perturbations," *Flow, Turbulence and Combustion*, Vol. 80, 2008, pp. 61–80.
doi:10.1007/s10494-007-9085-3

[5] Wygnanski, I., and Weisbrot, I., "On the Pairing Process in an Excited Plane Turbulent Mixing Layer," *Journal of Fluid Mechanics*, Vol. 195, 1988, pp. 161–173.
doi:10.1017/S0022112088002368

[6] Reynolds, W. C., and Hussain, A. K. M. F., "The Mechanics of an Organized Wave in Turbulent Shear Flow, Part 3, Theoretical Models and Comparisons with Experiments," *Journal of Fluid Mechanics*, Vol. 54, 1972, pp. 263–288.
doi:10.1017/S0022112072000679

[7] Gaster, M., Kit, E., and Wygnanski, I., "Large Scale Structures in a Forced Turbulent Mixing Layer," *Journal of Fluid Mechanics*, Vol. 150, 1985, pp. 23–39.
doi:10.1017/S0022112085000027

[8] Israel, D. M., "URANS and VLES: Using Conventional RANS Models for Time Dependent Flows," AIAA Paper 2006-3908, 2006.

[9] Brown, G. L., and Roshko, A., "On Density Effects and Large Structure in Turbulent Mixing Layers," *Journal of Fluid Mechanics*, Vol. 64, 1974, pp. 775–816.
doi:10.1017/S002211207400190X

[10] Winant, C. D., and Browand, F. K., "Vortex Pairing: the Mechanism of Turbulent Mixing-Layer Growth at Moderate Reynolds Numbers," *Journal of Fluid Mechanics*, Vol. 63, 1974, pp. 237–255.
doi:10.1017/S0022112074001121

[11] Rikanati, A., Alon, U., and Shvarts, D., "Vortex-Merger Statistical-Mechanics Model for the Late Time Self-Similar Evolution of the Kelvin–Helmholtz Instability," *Physics of Fluids*, Vol. 15, 2003, pp. 3776–3785.
doi:10.1063/1.1624837

[12] Browand, F. K., and Weidman, P. D., "Large Scales in the Developing Mixing Layer," *Journal of Fluid Mechanics*, Vol. 76, 1976, pp. 127–144.
doi:10.1017/S0022112076003169

T. Jackson
Associate Editor